

Training-free score-based diffusion for parameter-dependent stochastic dynamical systems

Minglei Yang^{a,*}, Sicheng He^b

^a*Fusion Energy Division, Oak Ridge National Laboratory, Oak Ridge, TN, USA*

^b*Department of Mechanical and Aerospace Engineering, University of Tennessee, Knoxville, TN, USA*

Abstract

Simulating parameter-dependent stochastic differential equations (SDEs) presents significant computational challenges, as separate high-fidelity simulations are typically required for each parameter value of interest. Despite the success of machine learning methods in learning SDE dynamics, existing approaches either require expensive neural network training for score function estimation or lack the ability to handle continuous parameter dependence. We present a training-free conditional diffusion model framework for learning stochastic flow maps of parameter-dependent SDEs, where both drift and diffusion coefficients depend on physical parameters. The key technical innovation is a joint kernel-weighted Monte Carlo estimator that approximates the conditional score function using trajectory data sampled at discrete parameter values, enabling interpolation across both state space and the continuous parameter domain. Once trained, the resulting generative model produces sample trajectories for any parameter value within the training range without retraining, significantly accelerating parameter studies, uncertainty quantification, and real-time filtering applications. The performance of the proposed approach is demonstrated via three numerical examples of increasing complexity, showing accurate approximation of conditional distributions across varying parameter values.

Keywords: Score-based diffusion models, parameter-dependent SDEs, stochastic flow maps, generative models, supervised learning

1. Introduction

Stochastic differential equations (SDEs) are fundamental mathematical models for describing dynamical systems subject to random fluctuations [1, 2]. They arise naturally in diverse scientific and engineering applications, including financial modeling and various physical systems [3, 4]. In many of these applications, the drift and diffusion coefficients of the

***Notice:** This manuscript has been authored by UT-Battelle, LLC, under contract DE-AC05-00OR22725 with the US Department of Energy (DOE). The US government retains and the publisher, by accepting the article for publication, acknowledges that the US government retains a nonexclusive, paid-up, irrevocable, worldwide license to publish or reproduce the published form of this manuscript, or allow others to do so, for US government purposes. DOE will provide public access to these results of federally sponsored research in accordance with the DOE Public Access Plan.

*Corresponding author

Email addresses: yangm@ornl.gov (Minglei Yang), sicheng@utk.edu (Sicheng He)

SDE depend on physical parameters that may vary across different operating conditions or experimental settings, such as diffusivity in transport processes or collision frequency in plasma physics. Understanding how these systems behave across a range of parameters is critical for uncertainty quantification (UQ), sensitivity analysis, and the design of reliable engineering systems [5].

The mathematical significance of SDEs lies in their ability to provide both a particle-based description through stochastic trajectories and a continuum description via the associated Fokker–Planck partial differential equation [6, 7, 8]. However, numerical solutions face substantial challenges in both formulations. Traditional particle-based methods, such as the Euler–Maruyama scheme and its high-order variants [9, 10], can become computationally prohibitive when long-time simulations or large ensembles of trajectories are required. This computational burden is further exacerbated when parameter studies are needed, as separate high-fidelity simulations must be performed for each parameter value of interest. Meanwhile, PDE-based approaches [11, 12] suffer from numerical instability, poor scalability with dimensions, and algorithmic challenges in parallelization.

Recently, machine learning (ML) approaches have emerged as promising alternatives for learning surrogate models of stochastic dynamics. Once trained, these models enable fast inference at new parameter values without requiring expensive repeated simulations, making them particularly attractive for parameter studies, uncertainty quantification, and integration with filtering frameworks such as differentiable Kalman filters [13]. These techniques span a broad spectrum, including Physics-informed neural networks [14, 15], Gaussian processes [16, 17], Flow Map Learning [18, 19], polynomial approximations [20], and generative models such as Normalizing Flows [21, 22, 23, 24].

Despite these successes, training generative models remains challenging due to mode collapse in GANs or architectural constraints in normalizing flows [25, 26]. Among various ML approaches, score-based diffusion models [27, 28, 29] have demonstrated remarkable success by learning the score function to generate samples through a reverse-time process. A training-free conditional diffusion model was developed in [30] for learning stochastic flow maps, where the exact score function admits a closed-form expression that can be estimated via Monte Carlo methods. Recent extensions have addressed SDEs in bounded domains via exit prediction networks [31] and developed multi-fidelity approaches for amortized Bayesian inference [32]. Error analysis in [33] shows that the analytically tractable score function avoids accumulation of approximation errors, with bounds scaling as $\mathcal{O}(d)$ in l^2 and $\mathcal{O}(\log d)$ in l^∞ .

In this work, we extend the training-free conditional diffusion framework to handle parameter-dependent SDEs where drift and diffusion coefficients depend on both the state and a physical parameter vector. The key technical innovation is a joint kernel-weighted Monte Carlo estimator that approximates the conditional score function using trajectory data sampled at discrete parameter values, enabling interpolation across both state space and the continuous parameter domain. We employ a two-stage procedure: the training-free score estimator first generates labeled training data via probability flow ODEs, then a feed-forward neural network is trained via supervised regression on this data. This converts the challenging unsupervised generative modeling problem into a standard supervised learning task with training stability and architectural flexibility. The resulting framework learns a unified model that produces sample trajectories across different parameter values, enabling

fast inference for parameter studies, uncertainty quantification, and real-time filtering.

The remainder of this paper is organized as follows. In Section 2, we introduce the parameter-dependent SDE formulation and the stochastic flow map representation. In Section 3, we present the training-free conditional diffusion framework, including the generative model formulation, training data from Monte Carlo simulations, and training-free score estimation. The algorithm and implementation details are described in Section 4. Numerical experiments are presented in Section 5, followed by conclusions in Section 6.

2. Problem formulation

We consider dynamical systems governed by parameter-dependent SDEs. The drift and diffusion coefficients depend on both the state and a parameter vector. This section introduces the mathematical framework, including the SDE formulation and the stochastic flow map that characterizes one-step transitions.

2.1. Parameter-dependent stochastic differential equations

We consider the following d -dimensional parameter-dependent SDE:

$$dX_t = a(X_t, \mu) dt + b(X_t, \mu) dW_t, \quad X_0 = x_0 \in \mathbb{R}^d, \quad (1)$$

where $X_t \in \mathbb{R}^d$ is the state variable, $x_0 \in \mathbb{R}^d$ is the initial condition, $\mu \in \mathcal{M} \subset \mathbb{R}^{d_\mu}$ is a parameter vector belonging to a parameter domain \mathcal{M} , $a : \mathbb{R}^d \times \mathbb{R}^{d_\mu} \rightarrow \mathbb{R}^d$ is the drift coefficient, $b : \mathbb{R}^d \times \mathbb{R}^{d_\mu} \rightarrow \mathbb{R}^{d \times m}$ is the diffusion coefficient, and $W_t \in \mathbb{R}^m$ is an m -dimensional standard Brownian motion. The parameter μ may represent various physical quantities depending on the application, e.g., diffusivity, or collision frequency [34, 35].

Assumption 2.1. We assume the following conditions hold for all $\mu \in \mathcal{M}$:

- (i) The functions $a(\cdot, \mu)$ and $b(\cdot, \mu)$ satisfy the global Lipschitz condition: there exists $L > 0$ such that for all $x, y \in \mathbb{R}^d$,

$$\|a(x, \mu) - a(y, \mu)\| + \|b(x, \mu) - b(y, \mu)\|_F \leq L\|x - y\|. \quad (2)$$

- (ii) The functions $a(\cdot, \mu)$ and $b(\cdot, \mu)$ satisfy the linear growth condition: there exists $K > 0$ such that for all $x \in \mathbb{R}^d$,

$$\|a(x, \mu)\| + \|b(x, \mu)\|_F \leq K(1 + \|x\|). \quad (3)$$

- (iii) The functions a and b are continuous in μ for each fixed x .

where $\|\cdot\|$ denotes the l^2 norm.

Under Assumption 2.1, for each initial condition x_0 and parameter μ , there exists a unique strong solution $\{X_t^{x_0, \mu}\}_{t \geq 0}$ to the SDE in Eq. (1) [1]. This ensures that the forward evolution is well-defined and that the conditional distributions we seek to learn are uniquely determined by the parameter value.

2.2. The stochastic flow map

To formulate the learning problem, we introduce a uniform temporal mesh

$$\mathcal{T} := \{t_n : t_n = n\Delta t, n = 0, 1, \dots, N_T\}, \quad (4)$$

where $T > 0$ is the final time, $N_T \in \mathbb{Z}^+$ is the number of time steps, and $\Delta t = T/N_T$ is the time step size. On each time interval $[t_n, t_{n+1}]$, the SDE in Eq. (1) can be written in the conditional form:

$$X_{t_{n+1}}^{t_n, x} = x + \int_{t_n}^{t_{n+1}} a(X_s^{t_n, x}, \mu) \, ds + \int_{t_n}^{t_{n+1}} b(X_s^{t_n, x}, \mu) \, dW_s, \quad (5)$$

where $X_{t_{n+1}}^{t_n, x}$ denotes the solution at time t_{n+1} conditioned on $X_{t_n} = x$. For notational simplicity, we denote $X_n := X_{t_n}$ and define the *stochastic flow map* $F_{\Delta t}$ such that

$$X_{n+1} = X_n + F_{\Delta t}(X_n, \mu, \omega), \quad (6)$$

where ω represents the randomness from the Brownian motion over the interval $[t_n, t_{n+1}]$.

Remark 2.2. The flow map $F_{\Delta t}(x, \mu, \omega)$ encapsulates the combined effects of drift, diffusion, and the parameter value μ . Unlike deterministic flow maps, this is a random variable for each fixed (x, μ) pair. In terms of (5), we have

$$F_{\Delta t}(x, \mu, \omega) = \int_{t_n}^{t_{n+1}} a(X_s^{t_n, x}, \mu) \, ds + \int_{t_n}^{t_{n+1}} b(X_s^{t_n, x}, \mu) \, dW_s. \quad (7)$$

This representation makes explicit the dependence on both the drift and diffusion terms integrated over the time interval.

The conditional distribution of X_{n+1} given $X_n = x_n$ and parameter μ , which we denote by

$$X_{n+1} \mid (X_n = x_n, \mu) \sim p(\cdot \mid x_n, \mu), \quad (8)$$

is the transition kernel of the Markov process parameterized by μ . Learning this parameter-dependent conditional distribution $p(\cdot \mid x_n, \mu)$ is the central objective of this work. The key challenge is to construct a generative model that accurately captures this distribution across the entire parameter domain \mathcal{M} , enabling efficient sampling for any parameter value μ without repeated expensive simulations.

3. Training-free conditional diffusion framework

Having defined the parameter-dependent SDE and its associated flow map, we now present the proposed method for learning the stochastic flow map. The methodology consists of four main components: (1) the generative model formulation; (2) training data from Monte Carlo simulations; (3) a training-free score estimation approach; and (4) a supervised learning framework for training the generative model. The approach extends the framework developed in [30, 36] to the parameter-dependent setting.

The term “training-free” in this work refers specifically to the score function estimation: unlike standard diffusion models that train neural networks to approximate the score function via score-matching losses, our approach derives a closed-form expression that can be directly estimated via Monte Carlo methods using trajectory data. The final stochastic flow map G_θ is subsequently learned through supervised regression on the diffusion-generated labeled data. This two-stage procedure converts the challenging unsupervised generative modeling problem into a standard supervised learning task.

3.1. Generative model for the stochastic flow map

To approximate the target distribution $p(\cdot \mid x_n, \mu)$, we aim to learn a parameterized generative model $G_\theta : \mathbb{R}^d \times \mathbb{R}^{d_\mu} \times \mathbb{R}^d \rightarrow \mathbb{R}^d$ such that

$$\hat{X}_{n+1} = X_n + G_\theta(X_n, \mu, Z), \quad Z \sim \mathcal{N}(0, I_d), \quad (9)$$

where $Z \in \mathbb{R}^d$ is a standard d -dimensional Gaussian random variable and $\theta \in \mathbb{R}^p$ denotes the neural network parameters with dimension p determined by the network architecture. The neural network G_θ serves as an approximation to the stochastic flow map $F_{\Delta t}$ defined in Eq. (6), replacing the abstract randomness ω with an explicit Gaussian latent variable z . The distribution of \hat{X}_{n+1} should match the true conditional distribution $p(\cdot \mid X_n, \mu)$ for all $(X_n, \mu) \in \mathbb{R}^d \times \mathcal{M}$.

The key challenge is that labeled training data of the form (x_n, μ, z, x_{n+1}) are not directly available from Monte Carlo simulations: while we can observe state transitions (x_n, x_{n+1}) for each parameter μ , the latent Gaussian variable z that maps to each specific x_{n+1} is unknown. We address this challenge by using a score-based diffusion model to generate such labeled data, forming an augmented dataset $\mathcal{D}_{\text{aug}} = \{(x_n, \mu, z, \hat{x}_{n+1})\}$.

3.2. Training data from Monte Carlo simulations

We assume access to trajectory data generated by Monte Carlo simulations of the SDE (1) at various parameter values. Specifically, let $N_\mu \in \mathbb{N}$ denote the number of parameter values and $N_s \in \mathbb{N}$ denote the number of trajectories per parameter. For a collection of parameter values $\{\mu^{(k)}\}_{k=1}^{N_\mu} \subset \mathcal{M}$, we simulate N_s independent trajectories for each parameter value, yielding the observed dataset

$$\mathcal{D}_{\text{obs}} = \left\{ \left(x_n^{(i,k)}, \mu^{(k)}, x_{n+1}^{(i,k)} \right) : i = 1, \dots, N_s, k = 1, \dots, N_\mu, n = 0, \dots, N_T - 1 \right\}. \quad (10)$$

For notational convenience, we reorganize this dataset as a collection of state transition pairs:

$$\mathcal{D}_{\text{obs}} = \left\{ (x_n^{(j)}, \mu^{(j)}, x_{n+1}^{(j)}) \right\}_{j=1}^J, \quad (11)$$

where $J = N_s \times N_\mu \times N_T$ is the total number of training pairs, $x_n^{(j)}$ and $x_{n+1}^{(j)}$ represent consecutive states, and $\mu^{(j)}$ is the associated parameter value. The central task is to generate the augmented dataset \mathcal{D}_{aug} from \mathcal{D}_{obs} ; the following subsections present a training-free diffusion approach to accomplish this.

3.3. Overview of the diffusion-based approach

We employ a score-based diffusion model to learn the parameter-dependent conditional distribution $p(x_{n+1} \mid x_n, \mu)$, which describes the transition probability from state x_n to x_{n+1} for each fixed parameter value μ . The key idea is to construct a diffusion process that transforms this conditional distribution into a standard Gaussian, and then reverse this process to generate samples. The framework builds upon score-based diffusion theory [37, 27], which we extend to handle parameter-dependent conditional distributions.

The approach consists of two stages:

- (i) *Forward diffusion*: Transform the conditional distribution $p(\cdot \mid x_n, \mu)$ into a standard Gaussian $\mathcal{N}(0, I_d)$ via a diffusion process on an artificial time domain $\tau \in [0, 1]$.
- (ii) *Reverse-time ODE*: Run the reverse process deterministically to map latent Gaussian samples $z \sim \mathcal{N}(0, I_d)$ back to samples from $p(\cdot \mid x_n, \mu)$.

The reverse-time process is governed by the *probability flow ODE*:

$$dZ_\tau^{x_n, \mu} = \left[f(\tau)Z_\tau^{x_n, \mu} - \frac{1}{2}g^2(\tau)S(Z_\tau^{x_n, \mu}, \tau; x_n, \mu) \right] d\tau, \quad (12)$$

where $f(\tau) = -1/(1 - \tau)$ and $g(\tau) = \sqrt{(1 + \tau)/(1 - \tau)}$ are the drift and diffusion coefficients of the variance-preserving (VP) forward process (see [Appendix A](#) for derivation), and $S(z, \tau; x_n, \mu)$ is the *parameter-dependent conditional score function*:

$$S(z, \tau; x_n, \mu) := \nabla_z \log Q(Z_\tau^{x_n, \mu} = z \mid x_n, \mu), \quad (13)$$

where $Q(Z_\tau^{x_n, \mu} = z \mid x_n, \mu)$ denotes the marginal density of the diffusion state at time τ conditioned on (x_n, μ) .

The diffusion process is applied to the *displacement* $\Delta X_{n+1} := X_{n+1} - X_n$ rather than the absolute state X_{n+1} . The ODE (12) thus establishes a deterministic mapping from $Z_1 \sim \mathcal{N}(0, I_d)$ to $Z_0 \sim p_\Delta(\cdot \mid x_n, \mu)$, where $p_\Delta(\cdot \mid x_n, \mu)$ denotes the conditional distribution of the displacement. This deterministic nature is crucial for generating labeled training data, as it establishes a one-to-one correspondence between each latent Gaussian variable z and its corresponding displacement Δx_{n+1} . Complete derivations of the forward and reverse diffusion processes are provided in [Appendix A](#).

3.4. Training-free score estimation

A key contribution of [30, 36] is the derivation of a closed-form expression for the conditional score function that can be estimated directly from data without training a neural network. We extend this approach to the parameter-dependent setting.

The score function in Eq. (13) can be expressed as a weighted average over the displacement distribution $p_\Delta(\Delta x \mid x_n, \mu)$ (see [Appendix B](#) for the complete derivation):

$$S(z, \tau; x_n, \mu) = \int_{\mathbb{R}^d} \left(-\frac{z - \alpha_\tau \Delta x}{\beta_\tau^2} \right) w_\tau(z, \Delta x; x_n, \mu) p_\Delta(\Delta x \mid x_n, \mu) d(\Delta x), \quad (14)$$

where $\alpha_\tau = 1 - \tau$ and $\beta_\tau^2 = \tau$ are the VP schedule scaling functions, and $\Delta x = x_{n+1} - x_n$ denotes the displacement. The weight function $w_\tau(z, \Delta x; x_n, \mu)$ favors displacement values

more likely to have produced the diffusion state z ; see [Appendix B](#) for its explicit form. This representation reveals that the score function is interpretable as a weighted average of “local scores” $-(z - \alpha_\tau \Delta x)/\beta_\tau^2$ over all possible displacement values.

Since the displacement distribution $p_\Delta(\Delta x \mid x_n, \mu)$ is unknown, we approximate the score function S in Eq. (14) via Monte Carlo estimation. In principle, if we had displacement samples $\{\Delta x^{(\ell)}\}_{\ell=1}^N$ drawn exactly from $p_\Delta(\cdot \mid x_n, \mu)$, we could approximate the score by replacing the integral with a sum and using the theoretical weights w_τ from Eq. (14). However, our dataset \mathcal{D}_{obs} contains samples from various (x_n, μ) pairs, not necessarily at the exact query point.

To address this, we select the N nearest neighbors of (x_n, μ) from \mathcal{D}_{obs} in the joint space, denoted $\{(x_n^{(j_\ell)}, \mu^{(j_\ell)}, x_{n+1}^{(j_\ell)})\}_{\ell=1}^N$, and compute the corresponding displacements $\Delta x^{(j_\ell)} = x_{n+1}^{(j_\ell)} - x_n^{(j_\ell)}$. The score function is then approximated by:

$$\bar{S}(z, \tau; x_n, \mu) := \sum_{\ell=1}^N \left(-\frac{z - \alpha_\tau \Delta x^{(j_\ell)}}{\beta_\tau^2} \right) \bar{w}_\tau^\ell, \quad (15)$$

where \bar{w}_τ^ℓ are the normalized Monte Carlo weights that approximate the theoretical weights w_τ in Eq. (14). Since the neighbor samples are not exactly at (x_n, μ) , we extend the theoretical weight (which only involves the Gaussian transition density $Q(z \mid \Delta x)$) by incorporating kernel density estimation for the proximity in both x_n and μ :

$$\bar{w}_\tau^\ell \propto \underbrace{\exp\left(-\frac{\|z - \alpha_\tau \Delta x^{(j_\ell)}\|^2}{2\beta_\tau^2}\right)}_{\text{diffusion weight } Q(z \mid \Delta x^{(j_\ell)})} \cdot \underbrace{\exp\left(-\frac{\|x_n - x_n^{(j_\ell)}\|^2}{2\nu_x^2}\right)}_{\text{spatial kernel}} \cdot \underbrace{\exp\left(-\frac{\|\mu - \mu^{(j_\ell)}\|^2}{2\nu_\mu^2}\right)}_{\text{parameter kernel}}, \quad (16)$$

with normalization $\sum_{\ell=1}^N \bar{w}_\tau^\ell = 1$. The first term corresponds to the theoretical weight w_τ derived in Eq. [Appendix B](#), while the spatial and parameter kernels account for the fact that neighbor samples originate from nearby but not identical (x_n, μ) values. Here, $\nu_x > 0$ and $\nu_\mu > 0$ are bandwidth parameters controlling the influence of spatial and parameter proximity, respectively. This joint kernel weighting approach naturally handles interpolation in both the state variable x_n and the parameter μ simultaneously, enabling generalization beyond the discrete training samples. When τ is small, $\beta_\tau^2 \approx 0$ causes the diffusion weights to become sharply peaked; in practice, we add a small regularization $\delta > 0$ to β_τ^2 for numerical stability.

4. Algorithm and implementation

The algorithm first generates labeled data by solving the probability flow ODE in Eq. (12), which establishes a deterministic mapping from latent space $Z_1 \sim \mathcal{N}(0, I_d)$ to the target distribution:

$$\mathcal{D}_{\text{aug}} = \left\{ (x_n^{(m)}, \mu^{(m)}, z^{(m)}, \hat{x}_{n+1}^{(m)}) \right\}_{m=1}^M. \quad (17)$$

The neural network G_θ is then trained via supervised learning to minimize the mean squared error (MSE) loss $\mathcal{L}(\theta)$ defined as

$$\mathcal{L}(\theta) = \frac{1}{M} \sum_{m=1}^M \left\| G_\theta(x_n^{(m)}, \mu^{(m)}, z^{(m)}) - (\hat{x}_{n+1}^{(m)} - x_n^{(m)}) \right\|^2, \quad (18)$$

Algorithm 1 Training-free conditional diffusion for parameter-dependent flow maps

Require: Observed dataset $\mathcal{D}_{\text{obs}} = \{(x_n^{(j)}, \mu^{(j)}, x_{n+1}^{(j)})\}_{j=1}^J$, number of labeled samples M , ODE time steps N_τ , number of neighbors N

Ensure: Trained generative model G_θ

```

1:  $\mathcal{D}_{\text{aug}} \leftarrow \emptyset$                                  $\triangleright$  Initialize augmented dataset
2: for  $m = 1, \dots, M$  do
3:    $(x_n^{(m)}, \mu^{(m)}) \sim \mathcal{D}_{\text{obs}}$                  $\triangleright$  Sample query point
4:    $z^{(m)} \sim \mathcal{N}(0, I_d)$                                  $\triangleright$  Sample latent variable
5:    $Z_{N_\tau} \leftarrow z^{(m)}$                                  $\triangleright$  Initialize ODE
6:   for  $k = N_\tau, N_\tau - 1, \dots, 1$  do
7:      $\tau_k \leftarrow k/N_\tau, \Delta\tau \leftarrow 1/N_\tau$            $\triangleright$  Diffusion time
8:      $\{(x_n^{(j_\ell)}, \mu^{(j_\ell)}, x_{n+1}^{(j_\ell)})\}_{\ell=1}^N \leftarrow \text{NEARESTNEIGHBOR}(x_n^{(m)}, \mu^{(m)}, N, \mathcal{D}_{\text{obs}})$   $\triangleright$  Neighbors in  $(x, \mu)$ 
9:      $\Delta x^{(j_\ell)} \leftarrow x_{n+1}^{(j_\ell)} - x_n^{(j_\ell)}$  for  $\ell = 1, \dots, N$            $\triangleright$  Compute displacements
10:     $\bar{S} \leftarrow \sum_{\ell=1}^N \bar{w}_{\tau_k}^\ell \cdot \left( -\frac{Z_k - (1 - \tau_k)\Delta x^{(j_\ell)}}{\tau_k} \right)$   $\triangleright$  Score (15), weights (16) with  $(x_n, \mu)$  kernels
11:     $Z_{k-1} \leftarrow Z_k - \Delta\tau [f(\tau_k)Z_k - \frac{1}{2}g^2(\tau_k)\bar{S}]$            $\triangleright$  Euler step (12)
12:  end for
13:   $\hat{x}_{n+1}^{(m)} \leftarrow x_n^{(m)} + Z_0$                                  $\triangleright$  Displacement  $Z_0$  plus initial state
14:   $\mathcal{D}_{\text{aug}} \leftarrow \mathcal{D}_{\text{aug}} \cup \{(x_n^{(m)}, \mu^{(m)}, z^{(m)}, \hat{x}_{n+1}^{(m)})\}$            $\triangleright$  Labeled data (17)
15: end for
16:  $G_\theta \leftarrow \text{InitNN}()$                                  $\triangleright$  Initialize neural network
17: repeat
18:    $\{(x_n^{(i)}, \mu^{(i)}, z^{(i)}, \hat{x}_{n+1}^{(i)})\}_i \subset \mathcal{D}_{\text{aug}}$            $\triangleright$  Sample mini-batch
19:    $\theta \leftarrow \theta - \eta \nabla_\theta \sum_i \|G_\theta(x_n^{(i)}, \mu^{(i)}, z^{(i)}) - (\hat{x}_{n+1}^{(i)} - x_n^{(i)})\|^2$            $\triangleright$  Gradient step (18)
20: until  $\mathcal{L}_{\text{val}}(\theta)$  converges                                 $\triangleright$  Early stopping
21: return  $G_\theta$ 

```

where training uses early stopping based on the validation loss $\mathcal{L}_{\text{val}}(\theta)$, computed analogously on a held-out subset of \mathcal{D}_{aug} . The main computational cost is the nearest neighbor search during labeled data generation; our implementation uses k -d trees in [38] for efficient neighbor queries. The ODE solving requires N_τ evaluations of the score function per labeled sample.

5. Numerical experiments

In this section, we present numerical experiments to validate the proposed method across three test problems of increasing complexity. Example 1 considers Brownian motion with parameter-dependent drift ($d = 1, d_\mu = 1$), where μ controls the drift coefficient, providing a validation case with known analytical solutions. Example 2 studies an Ornstein-Uhlenbeck (OU) process with parameter-dependent drift and diffusion ($d = 1, d_\mu = 1$), where μ appears in both coefficients and the stationary variance exhibits non-monotonic dependence on μ . Example 3 considers a two-dimensional OU process with rotation ($d = 2, d_\mu = 1$), demonstrating the method’s capability for multi-dimensional state spaces with coupled dynamics.

All experiments are implemented in PyTorch [39] and executed on a workstation with an NVIDIA GPU. The neural network G_θ uses a fully-connected architecture with tanh activation functions, trained using the Adam optimizer [40] with learning rate 0.001 and batch size 1024. Training employs early stopping with patience of 50 epochs based on validation loss, using a 90%/10% train/validation split. Specific hyperparameters (network size, number of labeled samples M , ODE steps N_τ , neighbors N , and bandwidth parameters ν_x, ν_μ) are tuned per example and reported in each subsection. Our implementation uses k -d trees [38] for efficient neighbor queries during label generation.

Remark 5.1 (Reproducibility). The source code for all numerical experiments is publicly available at https://github.com/mlmathphy/Diffusion_parameter_SDE. All results presented in this section are fully reproducible using the provided repository.

5.1. Example 1: Brownian motion with parameter-dependent drift

Consider the general SDE (1) with $d = m = 1$ and coefficients:

$$a(x, \mu) = \mu, \quad b(x, \mu) = 1, \quad (19)$$

where $\mu \in [-1, 1]$ is the drift parameter. This yields the one-dimensional SDE:

$$dX_t = \mu dt + dW_t, \quad X_0 = x_0, \quad (20)$$

where W_t is a standard Brownian motion. This example serves as a validation case since exact analytical solutions are available.

5.1.1. Exact solutions

For the SDE in Eq. (20), the exact solution is

$$X_t = X_0 + \mu t + W_t. \quad (21)$$

The one-step conditional distribution $p(X_{n+1} | X_n = x, \mu)$ is Gaussian:

$$p(X_{n+1} | X_n = x, \mu) = \mathcal{N}(x + \mu \Delta t, \Delta t), \quad (22)$$

with conditional mean and variance:

$$\mathbb{E}[X_{n+1} | X_n = x, \mu] = x + \mu\Delta t, \quad \text{Var}[X_{n+1} | X_n = x, \mu] = \Delta t. \quad (23)$$

The conditional mean depends linearly on both the initial state x and the drift parameter μ , while the variance depends only on the time step Δt .

For the terminal distribution at time T with a Gaussian initial condition $X_0 \sim \mathcal{N}(m_0, \sigma_0^2)$, the exact distribution is also Gaussian:

$$X_T \sim \mathcal{N}(m_0 + \mu T, \sigma_0^2 + T). \quad (24)$$

This follows from the fact that $X_T = X_0 + \mu T + W_T$, where X_0 and W_T are independent Gaussian random variables.

5.1.2. Training procedure

We generate training data by simulating the SDE in Eq. (20) using the Euler-Maruyama scheme with a fine time step $\delta t = 0.001$. The training dataset consists of consecutive state pairs (X_n, X_{n+1}) sampled at $N_\mu = 21$ uniformly spaced parameter values $\mu \in [-1, 1]$. For each parameter value, we simulate $N_s = 5000$ independent trajectories over the time interval $[0, T]$ with $T = 1.0$ and recording time step $\Delta t = 0.1$. The initial conditions are sampled uniformly from $[-5, 5]$, yielding a total of $J = 1,050,000$ training pairs.

Following Algorithm 1, we generate $M = 50,000$ labeled training samples using the training-free conditional diffusion model with $N = 2000$ nearest neighbors based on the combined distance in (x, μ) space. The probability flow ODE in Eq. (12) is solved using the explicit Euler scheme with $N_\tau = 1,000$ time steps. The bandwidth parameters for the Gaussian kernel weights are set to $\nu_x = 1.0$ for spatial proximity and $\nu_\mu = 0.5$ for parameter proximity. The generative model $G_\theta(x, \mu, z)$ is parameterized as a fully-connected neural network with input dimension 3, three hidden layers with 128 neurons each, and output dimension 1. The network predicts the scaled displacement $(\hat{x}_{n+1} - x_n) \cdot c_{\text{scale}}$ with $c_{\text{scale}} = 3.0$; this scaling normalizes the network output to approximately unit variance, improving training stability and convergence.

5.1.3. Results

Figure 1 shows the learned conditional distribution compared with the exact solution in Eq. (22). The left panel displays the probability density function $p(X_{n+1} | X_n = 2, \mu)$ for two parameter values $\mu = -0.5$ and $\mu = 0.5$. The exact conditional means are $2 + (-0.5)(0.1) = 1.95$ and $2 + (0.5)(0.1) = 2.05$, respectively, with conditional standard deviation $\sqrt{\Delta t} = \sqrt{0.1} \approx 0.316$ for both cases. The learned distributions (markers), estimated using kernel density estimation from 50,000 generated samples, closely match the exact Gaussian distributions (solid lines). The right panel shows the conditional mean $\mathbb{E}[X_{n+1} | X_n = 2, \mu]$ as a function of μ . The learned means (markers), computed from 10,000 samples per parameter value, accurately capture the linear dependence $x + \mu\Delta t$ predicted by the exact formula (solid line). Quantitatively, the maximum absolute error in the conditional mean is 0.006 (mean absolute error 0.002), and the maximum relative error in the conditional variance is 2.5% (mean relative error 1.1%).

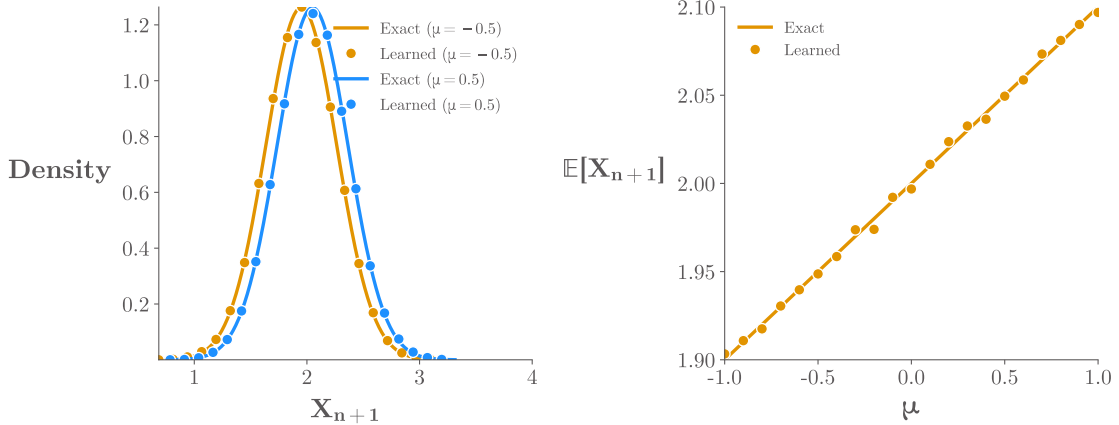


Figure 1: Example 1: Conditional distribution $p(X_{n+1} | X_n = 2, \mu)$. Left: PDF comparison for $\mu = -0.5$ and $\mu = 0.5$; solid lines show the exact Gaussian density (22), markers show learned estimates. Right: Conditional mean $\mathbb{E}[X_{n+1} | X_n = 2, \mu]$ vs. μ ; solid line is the exact formula $x + \mu\Delta t$, markers are learned estimates.

Figure 2 presents a heatmap comparison of the conditional distribution $p(X_{n+1} | X_n = 0, \mu)$ over the entire parameter range. The left panel shows the exact distribution computed from Eq. (22), and the right panel shows the learned distribution. The learned model accurately captures the shift in the distribution mean as μ varies from -1 to 1 . Notably, the model successfully interpolates to parameter values not included in the training set (which used $N_\mu = 21$ discrete values), demonstrating the method's ability to generalize across the continuous parameter space.

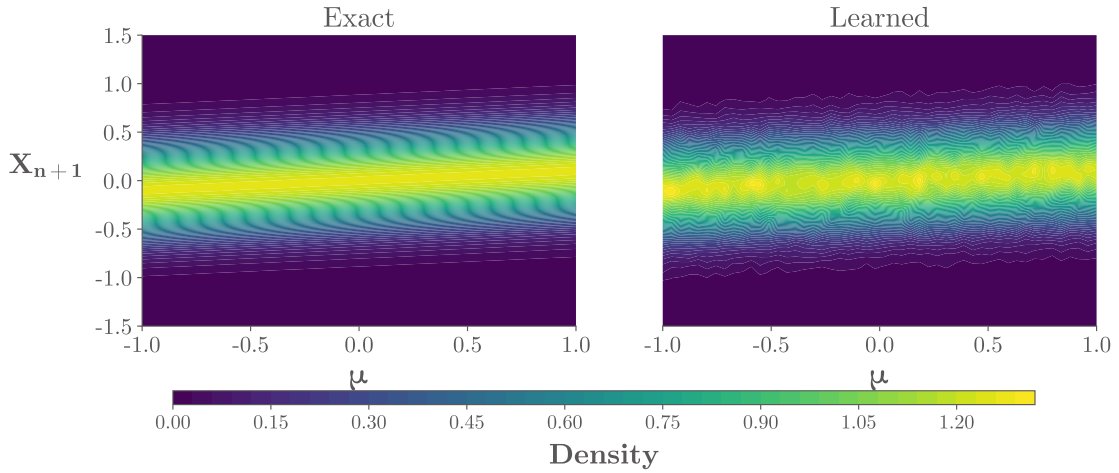


Figure 2: Example 1: Heatmap of conditional distribution $p(X_{n+1} | X_n = 0, \mu)$ over the parameter range $\mu \in [-1, 1]$. Left: Exact distribution from (22). Right: Learned distribution. The heatmaps are constructed using 5,000 samples per μ value. The learned model captures the linear shift in mean with μ .

To demonstrate the capability of multi-step prediction, Figure 3 shows the terminal distribution $p(X_T)$ at $T = 1.0$ starting from a non-delta initial distribution $X_0 \sim \mathcal{N}(0, 0.25)$. Multi-step trajectories are generated by iteratively applying the learned one-step flow map

with $N_{\text{steps}} = T/\Delta t = 10$ steps. The figure compares three approaches: (i) Monte Carlo ground truth using 50,000 samples from exact SDE simulation (solid lines), (ii) the analytical formula (24) (dashed lines), and (iii) our learned method using 50,000 generated trajectories (markers). The vertical dotted lines indicate the analytical mean $m_0 + \mu T$, which equals -0.5 for $\mu = -0.5$ (left panel) and 0.5 for $\mu = 0.5$ (right panel). According to (24), the terminal variance is $\sigma_0^2 + T = 0.25 + 1.0 = 1.25$ for both cases. The learned distributions closely match both the Monte Carlo reference and the analytical solution, validating the accuracy of the learned flow map for long-time prediction. Quantitatively, the terminal mean errors are below 0.006 and the terminal standard deviation errors are below 0.007 for both parameter values.

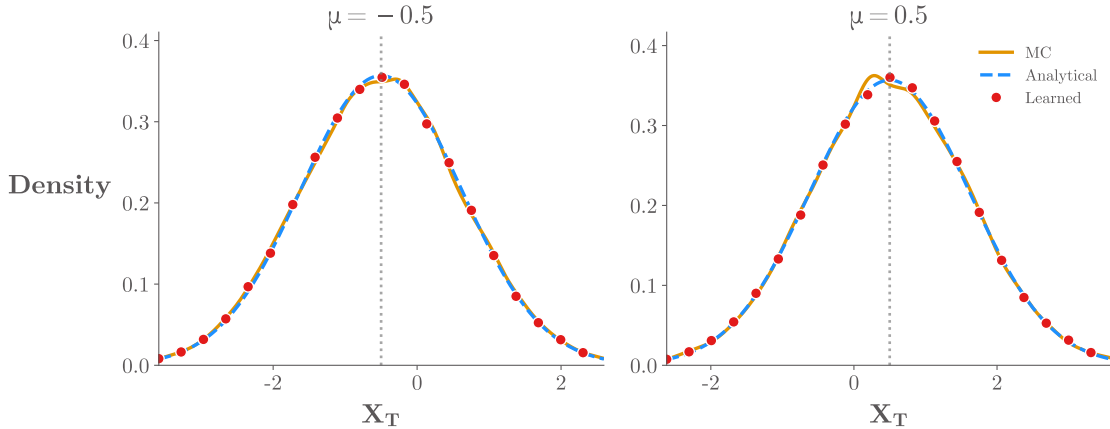


Figure 3: Example 1: Terminal distribution $p(X_T)$ at $T = 1.0$ with Gaussian initial distribution $X_0 \sim \mathcal{N}(0, 0.25)$, obtained via 10 iterative applications of the learned one-step flow map. Left panel: $\mu = -0.5$. Right panel: $\mu = 0.5$. Solid lines: Monte Carlo ground truth (50,000 samples); dashed lines: analytical formula (24); markers: learned method (50,000 generated trajectories). Vertical dotted lines indicate the analytical mean $m_0 + \mu T$.

5.2. Example 2: Ornstein-Uhlenbeck process with parameter-dependent drift and diffusion

To demonstrate the method's capability when the parameter appears in both drift and diffusion coefficients, we consider the general SDE (1) with $d = m = 1$ and coefficients:

$$a(x, \mu) = -\mu x, \quad b(x, \mu) = \sqrt{1 + \mu^2}, \quad (25)$$

where $\mu \in [0.5, 2]$ controls both the mean-reversion rate and the diffusion intensity. This yields the Ornstein-Uhlenbeck process:

$$dX_t = -\mu X_t dt + \sqrt{1 + \mu^2} dW_t, \quad X_0 = x_0. \quad (26)$$

This example is particularly interesting because the stationary variance exhibits non-monotonic dependence on μ .

5.2.1. Exact solutions

For the SDE (26), the exact solution is

$$X_t = X_0 e^{-\mu t} + \sqrt{1 + \mu^2} \int_0^t e^{-\mu(t-s)} dW_s. \quad (27)$$

The one-step conditional distribution $p(X_{n+1} | X_n = x, \mu)$ is Gaussian:

$$p(X_{n+1} | X_n = x, \mu) = \mathcal{N} \left(x e^{-\mu \Delta t}, \frac{1 + \mu^2}{2\mu} (1 - e^{-2\mu \Delta t}) \right), \quad (28)$$

with conditional mean and variance:

$$\mathbb{E}[X_{n+1} | X_n = x, \mu] = x e^{-\mu \Delta t}, \quad (29)$$

$$\text{Var}[X_{n+1} | X_n = x, \mu] = \frac{1 + \mu^2}{2\mu} (1 - e^{-2\mu \Delta t}). \quad (30)$$

The conditional mean exhibits exponential decay toward zero, while the variance depends on both μ and Δt through a more complex expression.

The stationary distribution is $\mathcal{N}(0, \sigma_\infty^2(\mu))$ with variance:

$$\sigma_\infty^2(\mu) = \frac{1 + \mu^2}{2\mu}. \quad (31)$$

Notably, this variance is non-monotonic in μ : it achieves its minimum value of 1 at $\mu = 1$, and increases for both $\mu < 1$ and $\mu > 1$.

For the terminal distribution at time T with a Gaussian initial condition $X_0 \sim \mathcal{N}(m_0, \sigma_0^2)$, the exact distribution is:

$$X_T \sim \mathcal{N} \left(m_0 e^{-\mu T}, \sigma_0^2 e^{-2\mu T} + \frac{1 + \mu^2}{2\mu} (1 - e^{-2\mu T}) \right). \quad (32)$$

This expression combines the exponential decay of the initial condition with the approach to the stationary distribution, and will be used to validate multi-step predictions.

5.2.2. Training procedure

We generate training data using the Euler-Maruyama scheme with fine time step $\delta t = 0.001$. The dataset consists of state pairs (X_n, X_{n+1}) at $N_\mu = 21$ uniformly spaced values $\mu \in [0.5, 2]$. For each parameter value, we simulate $N_s = 5000$ trajectories with recording time step $\Delta t = 0.1$ and total time $T = 1.0$. Initial conditions are sampled from the stationary distribution (31) for each μ , yielding a total of $J = 1,050,000$ training pairs. Following Algorithm 1, we generate $M = 20,000$ labeled samples using the training-free conditional diffusion model with $N = 1000$ nearest neighbors and $N_\tau = 500$ ODE time steps. The bandwidth parameters are $\nu_x = 1.0$ and $\nu_\mu = 0.3$, and the neural network architecture remains the same as in Example 1.

5.2.3. Results

Figure 4 shows the learned conditional distribution compared with the exact solution (28). The left panel displays the PDF $p(X_{n+1} | X_n = 1, \mu)$ for $\mu = 0.5$ and $\mu = 2.0$. The exact conditional means are $1 \cdot e^{-0.5 \cdot 0.1} \approx 0.951$ and $1 \cdot e^{-2 \cdot 0.1} \approx 0.819$, respectively. The mean-reversion effect is clearly visible: larger μ leads to stronger attraction toward zero (smaller conditional mean), while the diffusion coefficient $\sqrt{1 + \mu^2}$ also increases with μ . The learned distributions (markers) closely match the exact Gaussian distributions (solid lines). The right panel shows the conditional mean as a function of μ , demonstrating accurate capture of the exponential decay factor $e^{-\mu \Delta t}$. Quantitatively, the maximum relative error in the conditional mean is 1.4% (mean 0.6%), and the maximum relative error in the conditional variance is 2.8% (mean 1.6%).

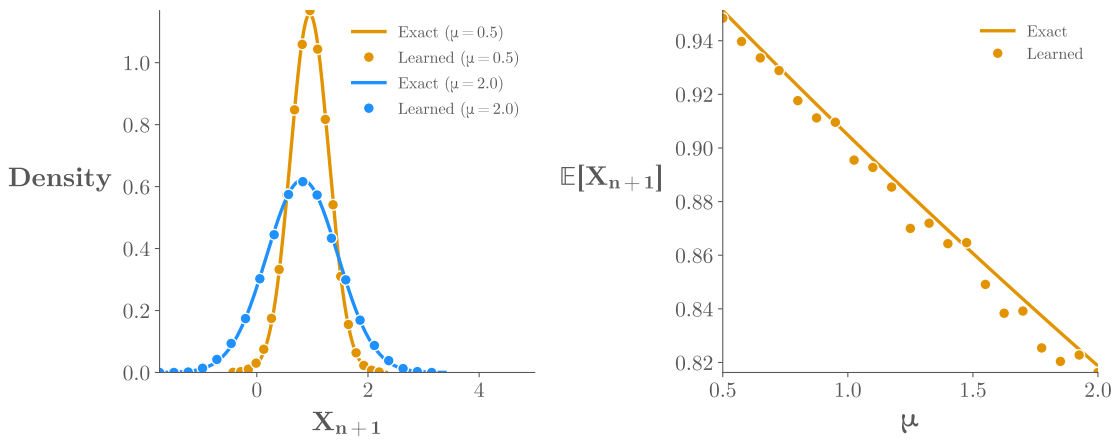


Figure 4: Example 2: Conditional distribution $p(X_{n+1} | X_n = 1, \mu)$. Left: PDF comparison for $\mu = 0.5$ and $\mu = 2.0$; solid lines show exact Gaussian density (28), markers show learned estimates. Right: Conditional mean $\mathbb{E}[X_{n+1} | X_n = 1, \mu]$ vs. μ ; solid line is the exact formula $xe^{-\mu \Delta t}$, markers are learned estimates.

Figure 5 presents a heatmap of the conditional distribution $p(X_{n+1} | X_n = 0, \mu)$ starting from the equilibrium point. The one-step conditional variance increases monotonically with μ , as seen from the increasing spread of the distribution from left to right. The learned model accurately captures this variance structure across the full parameter range.

Figure 6 shows the terminal distribution $p(X_T)$ at $T = 1.0$ starting from a non-equilibrium initial distribution $X_0 \sim \mathcal{N}(1.0, 0.25)$. Multi-step trajectories are generated using $N_{\text{steps}} = 10$ applications of the learned flow map. The figure compares three approaches: Monte Carlo ground truth (solid lines), analytical formula (32) (dashed lines), and our learned method (markers). The vertical dotted lines indicate the analytical mean $m_0 e^{-\mu T}$, which equals 0.607 for $\mu = 0.5$ and 0.135 for $\mu = 2.0$. The mean-reversion toward zero is clearly visible, with stronger reversion for larger μ . The learned distributions closely match both references, with terminal mean errors below 0.06 and standard deviation errors below 0.02.

Figure 7 quantifies the non-monotonic variance behavior that makes this example particularly interesting. The left panel shows the stationary variance $\sigma_\infty^2(\mu) = (1 + \mu^2)/(2\mu)$ as a function of μ , which achieves its minimum value of 1 at $\mu = 1$ (indicated by the vertical dotted line). The learned model accurately captures this non-monotonic structure after 50 time steps of evolution (50,000 samples per μ value), with maximum relative error 7.4%

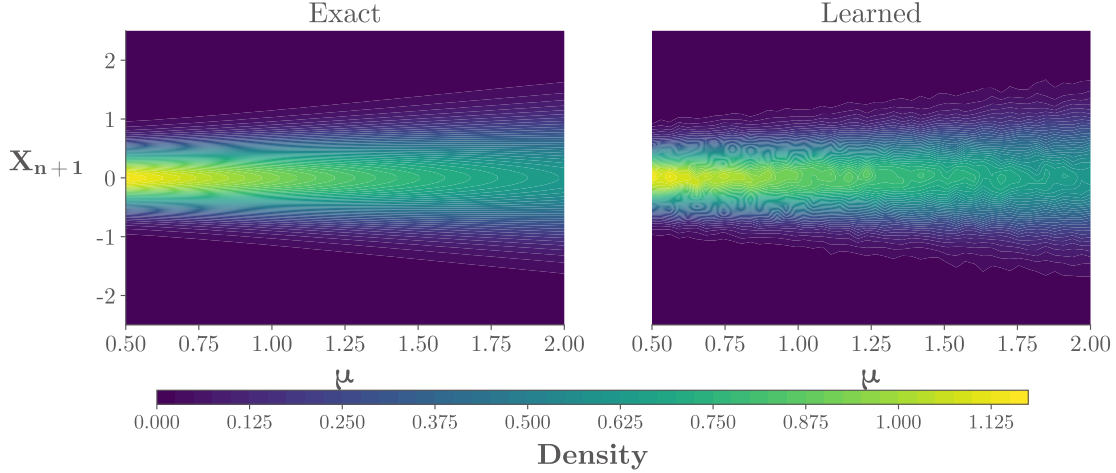


Figure 5: Example 2: Heatmap of conditional distribution $p(X_{n+1} | X_n = 0, \mu)$. Left: Exact. Right: Learned. The one-step conditional variance increases monotonically with μ . Constructed using 20,000 samples per μ value.

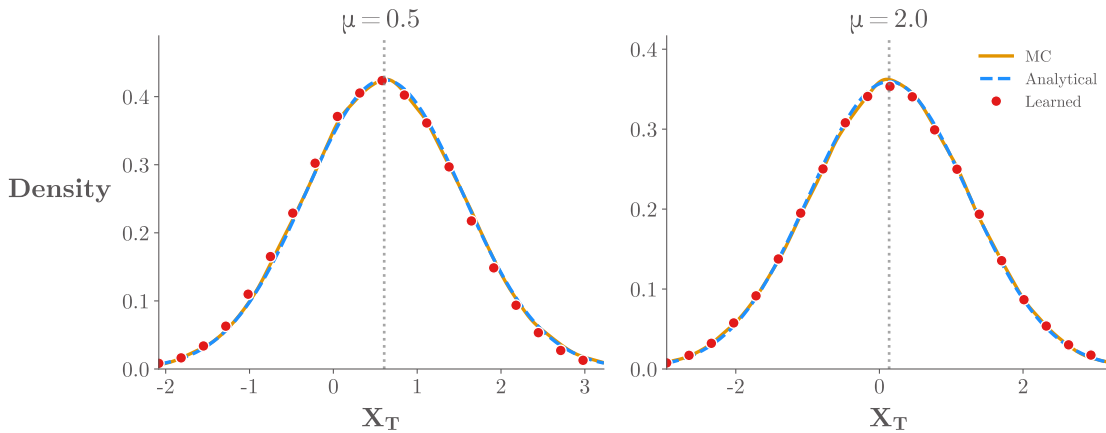


Figure 6: Example 2: Terminal distribution $p(X_T)$ at $T = 1.0$ with Gaussian initial distribution $X_0 \sim \mathcal{N}(1.0, 0.25)$, obtained via 10 iterative applications of the learned one-step flow map. Solid lines: Monte Carlo ground truth (50,000 samples); dashed lines: analytical formula (32); markers: learned method (50,000 generated trajectories). Vertical dotted lines indicate the analytical mean $m_0 e^{-\mu T}$.

(mean 1.6%). The right panel displays the one-step conditional variance, which increases monotonically with μ . The learned conditional variance has maximum relative error 3.4% (mean 1.7%). The excellent agreement between analytical and learned variances demonstrates that our method correctly captures both the mean and variance structure of the parameter-dependent dynamics.

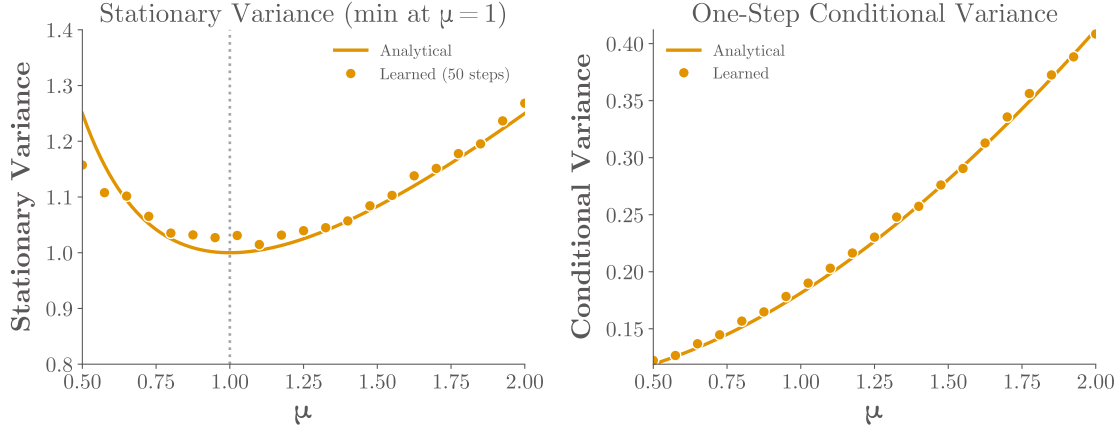


Figure 7: Example 2: Variance analysis. Left: Stationary variance $(1 + \mu^2)/(2\mu)$ showing non-monotonic behavior with minimum at $\mu = 1$ (vertical dashed line). Learned variance computed from 50,000 samples after 50 time steps. Right: One-step conditional variance from $X_n = 0$, comparing exact formula (28) with learned estimates (20,000 samples per μ value).

5.3. Example 3: Two-dimensional Ornstein-Uhlenbeck process with rotation

As a final example demonstrating the method’s capability in higher dimensions, we consider a two-dimensional Ornstein-Uhlenbeck process with rotation. This example showcases genuinely coupled 2D dynamics where the parameter controls both the decay rate and the spiral behavior of trajectories.

5.3.1. Problem formulation

Consider the general SDE (1) with $d = m = 2$ and coefficients:

$$a(x, \mu) = -Ax, \quad b(x, \mu) = \sigma I_2, \quad (33)$$

where $\sigma = 0.5$ and the drift matrix is:

$$A = \begin{pmatrix} \mu & -\omega \\ \omega & \mu \end{pmatrix}, \quad (34)$$

with $\mu \in [0.5, 2.0]$ being the decay rate parameter and $\omega = 1.0$ the fixed rotation frequency. This yields the two-dimensional SDE:

$$dX_t = -AX_t dt + \sigma dW_t, \quad X_0 = x_0 \in \mathbb{R}^2, \quad (35)$$

where W_t is a standard 2D Brownian motion. This matrix structure combines exponential decay (controlled by μ) with rotation (controlled by ω), resulting in spiral trajectories that converge to the origin.

5.3.2. Exact conditional statistics

The matrix exponential e^{-At} can be computed analytically:

$$e^{-At} = e^{-\mu t} \begin{pmatrix} \cos(\omega t) & \sin(\omega t) \\ -\sin(\omega t) & \cos(\omega t) \end{pmatrix}. \quad (36)$$

This factorization shows that trajectories undergo exponential decay at rate μ while simultaneously rotating at angular velocity ω .

The one-step conditional distribution is Gaussian:

$$\mathbb{E}[X_{n+1} | X_n = x, \mu] = e^{-A\Delta t} x, \quad (37)$$

$$\text{Cov}[X_{n+1} | X_n = x, \mu] = \frac{\sigma^2}{2\mu} (1 - e^{-2\mu\Delta t}) I_2. \quad (38)$$

Due to the isotropic noise structure, the covariance matrix is diagonal with equal variances in both dimensions, despite the asymmetric rotation dynamics.

5.3.3. Training procedure

We generate training data using exact sampling from the analytical transition distribution with $\Delta t = 0.1$, simulation time $T = 2.0$, $N_\mu = 16$ parameter values uniformly spaced in $[0.5, 2.0]$, and $N_s = 3000$ trajectories per parameter value, yielding approximately 960,000 training pairs in \mathbb{R}^2 .

Following Algorithm 1, we generate $M = 50,000$ labeled samples using $N = 2000$ nearest neighbors and $N_\tau = 500$ ODE time steps. Due to the higher dimensionality, we use a larger bandwidth $\nu_x = 0.8$ and $\nu_\mu = 0.3$, with scaling factor $c_{\text{scale}} = 3.0$. The neural network uses four hidden layers with 256 neurons each to accommodate the increased complexity of 2D dynamics.

5.3.4. Results

Figure 8 shows sample trajectories for three decay rates: $\mu = 0.5$ (slow decay), $\mu = 1.0$ (moderate decay), and $\mu = 2.0$ (fast decay). In all cases, trajectories spiral inward toward the origin due to the rotation term ω . The learned trajectories (dashed) closely follow the exact trajectories (solid), demonstrating that the model captures the coupled rotation-decay dynamics. Each panel reports the mean final radius $\bar{r} = \frac{1}{N} \sum_{i=1}^N \|X_T^{(i)}\|$, computed as the sample average of the Euclidean distance from the origin at the final time $T = 5$ over $N = 100$ trajectories. Larger μ leads to faster exponential decay, resulting in smaller \bar{r} . The close agreement between \bar{r}_{exact} (from exact simulations) and \bar{r}_{learned} (from the learned model) confirms that the learned model correctly captures the parameter-dependent decay rate.

Figure 9 shows the one-step conditional distribution starting from $x_0 = (1.5, 0.5)$ for three μ values. The top row shows exact samples from the analytical Gaussian distribution, and the bottom row shows learned samples. The learned model accurately captures both the location (mean) and spread (covariance) of the distribution, with the characteristic rotation visible in how the mean shifts relative to the starting point. From the conditional covariance formula (38), the one-step variance is approximately $\sigma^2 \Delta t$ for small Δt , but decreases with larger μ due to the factor $1/(2\mu)$. Quantitatively, the mean position error is below 0.024 and the relative variance error is below 3% for $\mu \leq 1$. For $\mu = 2$, the relative variance error

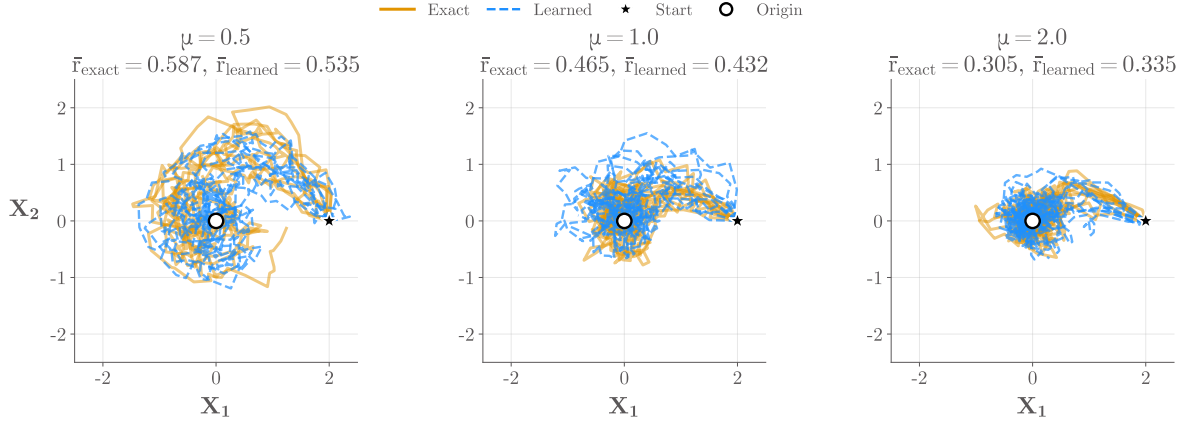


Figure 8: Example 3: Sample trajectories for 2D OU with rotation starting from $(2, 0)$ over $T = 5$. Left to right: $\mu = 0.5, 1.0, 2.0$. Solid lines: exact SDE trajectories; dashed lines: learned model trajectories. The mean final radius \bar{r} (averaged over 100 trajectories) measures convergence to the origin; larger μ leads to faster decay and smaller \bar{r} .

increases to 12.6%; however, this larger relative error reflects the smaller absolute variance at high μ (the conditional variance at $\mu = 2$ is approximately half that at $\mu = 0.5$), making relative errors more sensitive to small absolute differences.

Figure 10 compares the learned conditional mean with the exact formula (37) for three starting positions. The left panel shows the X_1 component and the right panel shows the X_2 component. The learned means (markers) closely track the exact curves (solid lines) across the full parameter range, demonstrating accurate learning of the rotation dynamics. The maximum absolute error in the conditional mean is below 0.05 for all starting positions and parameter values.

Figure 11 shows the multi-step behavior. The left panel displays the marginal distribution of X_1 at time $T = 2$ for three μ values. The learned distributions (markers) closely match the exact Monte Carlo distributions (solid lines). The right panel shows the variance evolution over time starting from a deterministic initial condition. Variance grows from zero toward the stationary value $\sigma^2/(2\mu)$, which is 0.25 for $\mu = 0.5$, 0.125 for $\mu = 1.0$, and 0.0625 for $\mu = 2.0$. The learned variance trajectories (markers) accurately track the exact analytical curves (solid lines), demonstrating that the model correctly captures the parameter-dependent diffusion dynamics. For the terminal distribution, the mean error is below 0.04 and the relative variance error is below 8%.

This example demonstrates that the proposed method scales effectively to multi-dimensional SDEs with coupled dynamics. The learned model captures both the rotational structure (from the off-diagonal terms in A) and the parameter-dependent decay rate, producing accurate samples from the joint 2D conditional distribution.

6. Conclusion

This work presents a training-free conditional diffusion framework for learning stochastic flow maps of parameter-dependent SDEs of the form $dX_t = a(X_t, \mu) dt + b(X_t, \mu) dW_t$. The key innovation lies in extending the training-free score estimation approach of [30, 31] to

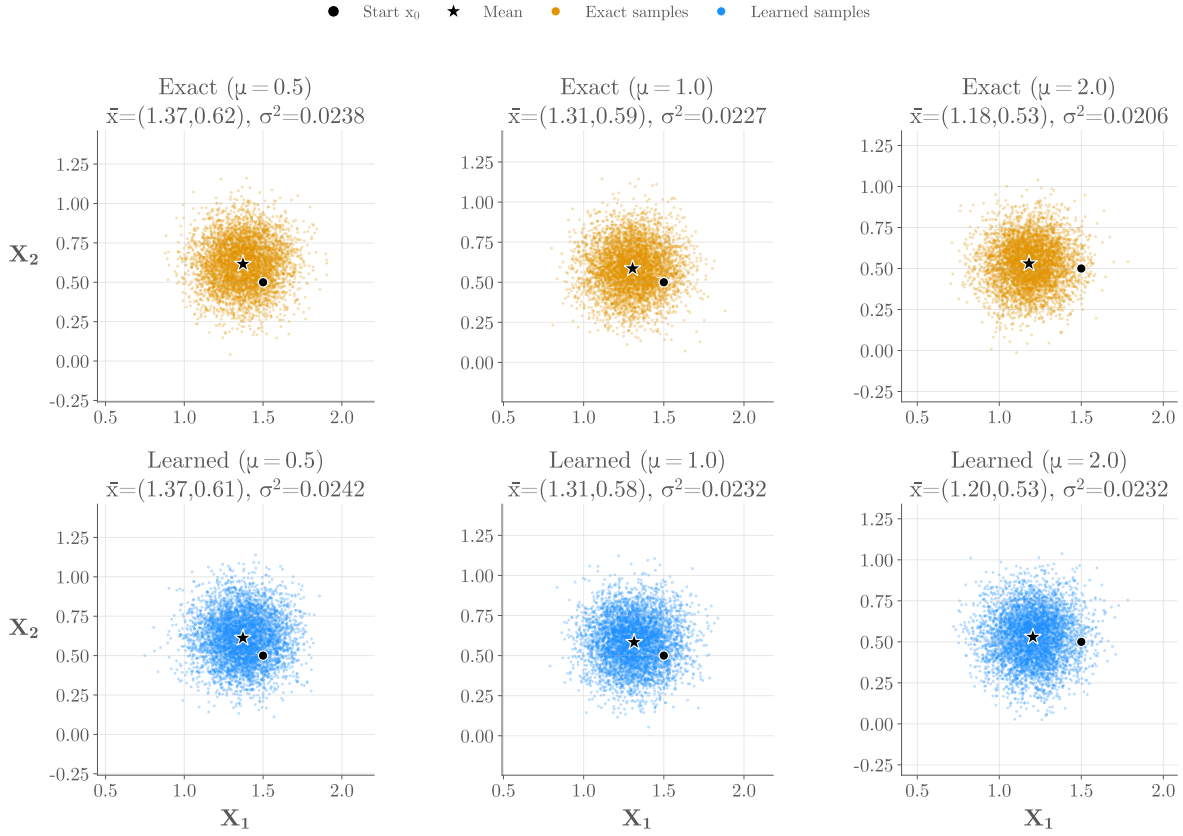


Figure 9: Example 3: One-step conditional distribution scatter plots starting from $(1.5, 0.5)$. Top row: exact samples from analytical Gaussian (37)–(38). Bottom row: learned model samples (5,000 samples each). Left to right: $\mu = 0.5, 1.0, 2.0$. Stars indicate the conditional mean; black dots indicate the starting position x_0 .

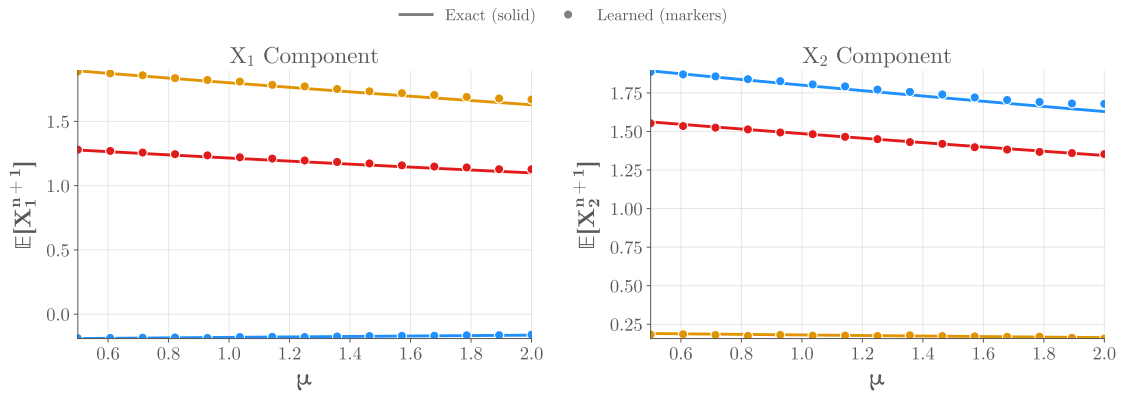


Figure 10: Example 3: Conditional mean comparison for 2D OU with rotation. Left: X_1 component. Right: X_2 component. Solid lines: exact formula (37). Markers: learned estimates (5,000 samples per point). Three starting positions are shown: $(2, 0)$, $(0, 2)$, and $(1.5, 1.5)$.

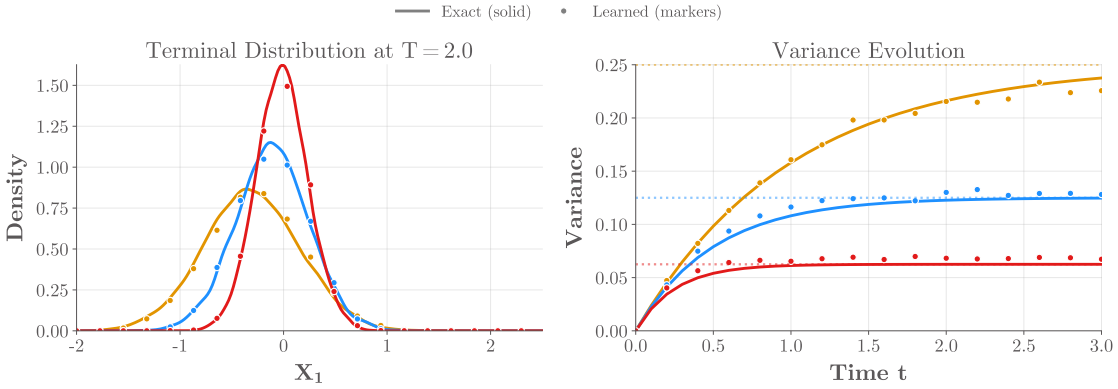


Figure 11: Example 3: Multi-step distribution and variance analysis. Left: Marginal distribution of X_1 at $T = 2$ for $\mu = 0.5, 1.0, 2.0$. Right: Variance evolution over time starting from deterministic initial condition $x_0 = (2, 0)$. Variance grows from zero toward the stationary variance $\sigma^2/(2\mu)$, which depends strongly on μ . Solid lines: exact analytical formula; markers: learned model.

handle parameter dependence, where the conditional score function is approximated using Gaussian kernel-weighted combinations of empirical displacements. This enables efficient generation of labeled training data for neural network regression without solving a computationally expensive score-matching optimization problem, which is particularly advantageous when exploring large parameter spaces.

Our methodology offers several distinct advantages for learning parameter-dependent stochastic dynamics. The training-free score estimation eliminates the computational overhead associated with neural network-based score function learning, replacing it with a closed-form Monte Carlo estimator that directly uses trajectory data. By incorporating parameter dependence through kernel weighting in both spatial and parameter dimensions, the framework learns a unified model that captures how the conditional distribution varies with the parameter μ , rather than requiring separate models for each parameter value. The two-stage approach—first generating labeled data via probability flow ODE, then training a simple neural network via supervised regression—provides training stability and architectural flexibility that would be difficult to achieve with end-to-end generative model training.

We demonstrate the framework’s effectiveness through comprehensive validation across three benchmark problems of increasing complexity. The parameter-dependent Brownian motion (Example 1) validates the basic methodology, with the learned model achieving mean absolute errors below 0.006 for the conditional mean and relative errors below 3.5% for the conditional variance across the entire parameter range. The Ornstein-Uhlenbeck process with parameter-dependent diffusion (Example 2) tests the method’s ability to capture non-trivial parameter dependence, where the stationary variance exhibits non-monotonic behavior as a function of the mean-reversion rate; the learned model reproduces this behavior with relative variance errors below 3.5%. The two-dimensional OU process with rotation (Example 3) extends the validation to multi-dimensional coupled dynamics, where the learned model captures both the rotational structure from off-diagonal drift terms and the parameter-dependent decay rate, achieving conditional mean errors below 1.5%. In all cases, multi-step trajectory generation via composition of single-step flow maps produces accurate long-time statistics, including terminal distributions and time-dependent variance evolution, confirming

the method’s ability to generalize beyond single-step predictions.

Future work will focus on extending the framework to higher-dimensional systems, which will require developing more efficient strategies for kernel density estimation and neighbor search. Additionally, we will investigate adaptive strategies for selecting the bandwidth parameters ν_x and ν_μ ; connections to optimal bandwidth selection in kernel density estimation may provide theoretical guidance for automatic tuning. Theoretical analysis of the approximation error introduced by the training-free score estimation would establish rigorous bounds on the learned flow map accuracy. Finally, the learned stochastic flow maps could serve as surrogate models in data assimilation frameworks, where accurate parameter-dependent dynamics are essential for state estimation in systems with uncertain parameters.

Acknowledgments

This material is based upon work supported in part by the U.S. Department of Energy, Office of Science, Offices of Advanced Scientific Computing Research and Fusion Energy Science, and by the Laboratory Directed Research and Development program at the Oak Ridge National Laboratory, which is operated by UT-Battelle, LLC, for the U.S. Department of Energy under Contract DE-AC05-00OR22725. S. He acknowledges support from the University of Tennessee, Knoxville AI seed grant.

References

- [1] B. Øksendal, Stochastic differential equations, in: Stochastic differential equations: an introduction with applications, Springer, 2003, pp. 38–50.
- [2] R. Khasminskii, Stochastic stability of differential equations, Springer, 2012.
- [3] E. Platen, N. Bruti-Liberati, Numerical solution of stochastic differential equations with jumps in finance, Vol. 64, Springer Science & Business Media, 2010.
- [4] K. Sobczyk, Stochastic differential equations: with applications to physics and engineering, Vol. 40, Springer Science & Business Media, 2013.
- [5] M. Grigoriu, Stochastic systems: uncertainty quantification and propagation, Springer Science & Business Media, 2012.
- [6] V. I. Kolobov, Fokker–planck modeling of electron kinetics in plasmas and semiconductors, Computational materials science 28 (2) (2003) 302–320.
- [7] A. G. Peeters, D. Strintzi, The fokker-planck equation, and its application in plasma physics, Annalen der Physik 520 (2-3) (2008) 142–157.
- [8] M. Yang, D. del Castillo-Negrete, G. Zhang, An efficient probabilistic scheme for the exit time probability of alpha-stable levy process, arXiv preprint arXiv:2601.09882 (2026).
- [9] C. Yuan, X. Mao, Convergence of the euler–maruyama method for stochastic differential equations with markovian switching, Mathematics and Computers in Simulation 64 (2) (2004) 223–235.

- [10] M. J. Piggott, V. Solo, Geometric euler–maruyama schemes for stochastic differential equations in $so(n)$ and $se(n)$, *SIAM Journal on Numerical Analysis* 54 (4) (2016) 2490–2516.
- [11] F. Liu, V. Anh, I. Turner, Numerical solution of the space fractional fokker–planck equation, *Journal of Computational and Applied Mathematics* 166 (1) (2004) 209–219.
- [12] P. Patie, C. Winter, First exit time probability for multidimensional diffusions: A pde-based approach, *Journal of computational and applied mathematics* 222 (1) (2008) 42–53.
- [13] Y. Wu, S. He, DKFNet: Differentiable Kalman filter for field inversion and machine learning, *arXiv preprint arXiv:2509.07474* (2025).
- [14] L. Yang, D. Zhang, G. E. Karniadakis, Physics-informed generative adversarial networks for stochastic differential equations, *SIAM Journal on Scientific Computing* 42 (1) (2020) A292–A317.
- [15] X. Chen, L. Yang, J. Duan, G. E. Karniadakis, Solving inverse stochastic problems from discrete particle observations using the fokker–planck equation and physics-informed neural networks, *SIAM Journal on Scientific Computing* 43 (3) (2021) B811–B830.
- [16] C. Archambeau, D. Cornford, M. Opper, J. Shawe-Taylor, Gaussian process approximations of stochastic differential equations, in: *Gaussian Processes in Practice*, PMLR, 2007, pp. 1–16.
- [17] M. Opper, Variational inference for stochastic differential equations, *Annalen der Physik* 531 (3) (2019) 1800233.
- [18] J. Chen, K. Wu, D. Xiu, Due: A deep learning framework and library for modeling unknown equations, *SIAM Review* 67 (4) (2025) 873–902.
- [19] Y. Chen, D. Xiu, Learning stochastic dynamical system via flow map operator, *Journal of Computational Physics* 508 (2024) 112984.
- [20] S. W. Werner, B. Peherstorfer, On the sample complexity of stabilizing linear dynamical systems from data, *Foundations of Computational Mathematics* 24 (3) (2024) 955–987.
- [21] M. S. Albergo, E. Vanden-Eijnden, Building normalizing flows with stochastic interpolants, *arXiv preprint arXiv:2209.15571* (2022).
- [22] M. Yang, P. Wang, D. del Castillo-Negrete, Y. Cao, G. Zhang, A pseudoreversible normalizing flow for stochastic dynamical systems with various initial distributions, *SIAM Journal on Scientific Computing* 46 (4) (2024) C508–C533.
- [23] J. Urain, M. Ginesi, D. Tateo, J. Peters, Imitationflow: Learning deep stable stochastic dynamic systems by normalizing flows, in: *2020 IEEE/RSJ International Conference on Intelligent Robots and Systems (IROS)*, IEEE, 2020, pp. 5231–5237.

- [24] M. Yang, P. Wang, M. Fan, D. Lu, Y. Cao, G. Zhang, Conditional pseudo-reversible normalizing flow for surrogate modeling in quantifying uncertainty propagation, *Journal of Machine Learning for Modeling and Computing* 6 (4) (2025).
- [25] T. Salimans, I. Goodfellow, W. Zaremba, V. Cheung, A. Radford, X. Chen, Improved techniques for training gans, *Advances in neural information processing systems* 29 (2016).
- [26] I. Kobyzev, S. J. Prince, M. A. Brubaker, Normalizing flows: An introduction and review of current methods, *IEEE transactions on pattern analysis and machine intelligence* 43 (11) (2020) 3964–3979.
- [27] Y. Song, J. Sohl-Dickstein, D. P. Kingma, A. Kumar, S. Ermon, B. Poole, Score-based generative modeling through stochastic differential equations, *International Conference on Learning Representations* (2021).
- [28] A. Q. Nichol, P. Dhariwal, Improved denoising diffusion probabilistic models, in: *International conference on machine learning*, PMLR, 2021, pp. 8162–8171.
- [29] L. Yang, Z. Zhang, Y. Song, S. Hong, R. Xu, Y. Zhao, W. Zhang, B. Cui, M.-H. Yang, Diffusion models: A comprehensive survey of methods and applications, *ACM computing surveys* 56 (4) (2023) 1–39.
- [30] Y. Liu, Y. Chen, D. Xiu, G. Zhang, A training-free conditional diffusion model for learning stochastic dynamical systems, *SIAM Journal on Scientific Computing* 47 (5) (2025) C1144–C1171.
- [31] M. Yang, Y. Liu, D. Del-Castillo-Negrete, Y. Cao, G. Zhang, Generative ai models for learning flow maps of stochastic dynamical systems in bounded domains, *Journal of Computational Physics* (2025) 114434.
- [32] C. Tatsuoka, M. Yang, D. Xiu, G. Zhang, Multi-fidelity parameter estimation using conditional diffusion models, *arXiv preprint arXiv:2504.01894* (2025).
- [33] P. Wang, Z. Zhang, M. Yang, F. Bao, Y. Cao, G. Zhang, Error estimates of a training-free diffusion model for high-dimensional sampling, *arXiv preprint arXiv:2601.19740* (2026).
- [34] Z. Wang, J. Xin, Z. Zhang, Computing effective diffusivity of chaotic and stochastic flows using structure-preserving schemes, *SIAM Journal on Numerical Analysis* 56 (4) (2018) 2322–2344.
- [35] A. V. Nguyen, D.-A. An-Vo, T. Tran-Cong, G. M. Evans, A review of stochastic description of the turbulence effect on bubble-particle interactions in flotation, *International Journal of Mineral Processing* 156 (2016) 75–86.
- [36] Y. Liu, M. Yang, Z. Zhang, F. Bao, Y. Cao, G. Zhang, Diffusion-model-assisted supervised learning of generative models for density estimation, *Journal of Machine Learning for Modeling and Computing* 5 (1) (2024).

- [37] B. D. Anderson, Reverse-time diffusion equation models, *Stochastic Processes and their Applications* 12 (3) (1982) 313–326.
- [38] J. L. Bentley, Multidimensional binary search trees used for associative searching, *Communications of the ACM* 18 (9) (1975) 509–517.
- [39] A. Paszke, S. Gross, F. Massa, A. Lerer, J. Bradbury, G. Chanan, T. Killeen, Z. Lin, N. Gimelshein, L. Antiga, et al., Pytorch: An imperative style, high-performance deep learning library, in: *Advances in Neural Information Processing Systems*, Vol. 32, 2019, pp. 8026–8037.
- [40] D. P. Kingma, J. Ba, Adam: A method for stochastic optimization, arXiv preprint arXiv:1412.6980 (2014).
- [41] J. Ho, A. Jain, P. Abbeel, Denoising diffusion probabilistic models, in: *Advances in Neural Information Processing Systems*, Vol. 33, 2020, pp. 6840–6851.

Appendix A. Forward and reverse diffusion processes

This appendix provides the theoretical foundations for the parameter-dependent conditional diffusion model used in Section 3.

Appendix A.1. Forward diffusion process

For a fixed pair (x_n, μ) , let $\Delta X_{n+1}^{x_n, \mu} = X_{n+1}^{x_n, \mu} - x_n$ denote the displacement, where $X_{n+1}^{x_n, \mu} \sim p(\cdot | x_n, \mu)$ follows the conditional distribution. Following [30], we define a forward diffusion process on the displacement in an artificial domain $\tau \in [0, 1]$:

$$dZ_\tau^{x_n, \mu} = f(\tau)Z_\tau^{x_n, \mu} d\tau + g(\tau) dW_\tau, \quad Z_0^{x_n, \mu} = \Delta X_{n+1}^{x_n, \mu}, \quad (\text{A.1})$$

where W_τ is a standard Brownian motion (independent of the original SDE), and $f(\tau)$ and $g(\tau)$ are the drift and diffusion coefficients of the forward diffusion process.

We choose the coefficients such that the forward process has an analytically tractable transition density. Specifically, we parameterize the solution of (A.1) as

$$Z_\tau^{x_n, \mu} = \alpha_\tau Z_0^{x_n, \mu} + \beta_\tau \epsilon, \quad \epsilon \sim \mathcal{N}(0, I_d), \quad (\text{A.2})$$

where α_τ and β_τ are deterministic scaling functions satisfying $\alpha_0 = 1$, $\beta_0 = 0$. For this parameterization to be consistent with (A.1), the coefficients must satisfy:

$$f(\tau) = \frac{d \log \alpha_\tau}{d\tau}, \quad g^2(\tau) = \frac{d \beta_\tau^2}{d\tau} - 2 \frac{d \log \alpha_\tau}{d\tau} \beta_\tau^2. \quad (\text{A.3})$$

These relations ensure that the marginal distribution of Z_τ follows the prescribed scaling.

In this work, we adopt the variance-preserving (VP) schedule [41]:

$$\alpha_\tau = 1 - \tau, \quad \beta_\tau^2 = \tau, \quad \tau \in [0, 1]. \quad (\text{A.4})$$

With this choice, we have $\alpha_1 = 0$ and $\beta_1 = 1$, so that $Z_1^{x_n, \mu} \sim \mathcal{N}(0, I_d)$ regardless of the initial displacement distribution $p_\Delta(\cdot | x_n, \mu)$.

From (A.2), the conditional distribution of $Z_\tau^{x_n, \mu}$ given $Z_0^{x_n, \mu} = \Delta x$ is Gaussian:

$$Q(Z_\tau^{x_n, \mu} \mid Z_0^{x_n, \mu} = \Delta x) = \mathcal{N}(\alpha_\tau \Delta x, \beta_\tau^2 I_d). \quad (\text{A.5})$$

This result follows directly from the linearity of (A.2): given $Z_0^{x_n, \mu} = \Delta x$, we have $Z_\tau^{x_n, \mu} = \alpha_\tau \Delta x + \beta_\tau \epsilon$ where $\epsilon \sim \mathcal{N}(0, I_d)$, yielding a Gaussian with mean $\alpha_\tau \Delta x$ and covariance $\beta_\tau^2 I_d$.

Appendix A.2. Reverse-time SDE and ODE

The key result from score-based diffusion theory is that the forward diffusion process (A.1) has a corresponding reverse-time process. Running the reverse process from $\tau = 1$ to $\tau = 0$ transforms samples from $\mathcal{N}(0, I_d)$ back to samples from the target displacement distribution $p_\Delta(\cdot \mid x_n, \mu)$.

Following [37], the reverse-time SDE is

$$dZ_\tau^{x_n, \mu} = [f(\tau)Z_\tau^{x_n, \mu} - g^2(\tau)S(Z_\tau^{x_n, \mu}, \tau; x_n, \mu)] d\tau + g(\tau) d\overleftarrow{W}_\tau, \quad (\text{A.6})$$

where \overleftarrow{W}_τ is a backward Brownian motion, and $S(z, \tau; x_n, \mu)$ is the parameter-dependent conditional score function defined in (13). Note that the score function depends on four quantities: the diffusion state z , the diffusion time τ , the initial state x_n , and the parameter μ ; the dependence on μ is the key extension from the standard conditional diffusion model in [30].

An important observation from [27] is that the reverse-time SDE (A.6) shares the same marginal distributions $Q(Z_\tau^{x_n, \mu} \mid x_n, \mu)$ with the deterministic probability flow ODE (12) presented in Section 3. The ODE defines a deterministic mapping from $Z_1 \sim \mathcal{N}(0, I_d)$ to $Z_0 \sim p_\Delta(\cdot \mid x_n, \mu)$, which is essential for generating labeled training data with a one-to-one correspondence between latent variables and displacement outputs.

Appendix B. Score function derivation

This appendix provides the complete derivation of the closed-form expression for the parameter-dependent conditional score function used in Section 3.

The marginal density of $Z_\tau^{x_n, \mu}$ conditioned on (x_n, μ) can be obtained by integrating over all possible initial displacement values:

$$Q(Z_\tau^{x_n, \mu} = z \mid x_n, \mu) = \int_{\mathbb{R}^d} Q(Z_\tau^{x_n, \mu} = z \mid Z_0^{x_n, \mu} = \Delta x) p_\Delta(\Delta x \mid x_n, \mu) d(\Delta x). \quad (\text{B.1})$$

Substituting the Gaussian transition density (A.5), we have

$$Q(z \mid x_n, \mu) = \int_{\mathbb{R}^d} \frac{1}{(2\pi\beta_\tau^2)^{d/2}} e^{-\frac{\|z - \alpha_\tau \Delta x\|^2}{2\beta_\tau^2}} p_\Delta(\Delta x \mid x_n, \mu) d(\Delta x). \quad (\text{B.2})$$

This integral representation expresses the marginal density as a mixture of Gaussians weighted by the displacement distribution $p_\Delta(\Delta x \mid x_n, \mu)$.

To derive the score function, we apply the log-derivative:

$$S(z, \tau; x_n, \mu) = \nabla_z \log Q(z \mid x_n, \mu) = \frac{\nabla_z Q(z \mid x_n, \mu)}{Q(z \mid x_n, \mu)}. \quad (\text{B.3})$$

Taking the gradient of (B.2) with respect to z :

$$\nabla_z Q(z \mid x_n, \mu) = \int_{\mathbb{R}^d} \left(-\frac{z - \alpha_\tau \Delta x}{\beta_\tau^2} \right) Q(z \mid \Delta x) p_\Delta(\Delta x \mid x_n, \mu) d(\Delta x), \quad (\text{B.4})$$

where $Q(z \mid \Delta x) := Q(Z_\tau^{x_n, \mu} = z \mid Z_0^{x_n, \mu} = \Delta x) = \mathcal{N}(z; \alpha_\tau \Delta x, \beta_\tau^2 I_d)$.

Substituting (B.2) and (B.4) into (B.3), we obtain the exact score function:

$$S(z, \tau; x_n, \mu) = \frac{\int_{\mathbb{R}^d} \left(-\frac{z - \alpha_\tau \Delta x}{\beta_\tau^2} \right) Q(z \mid \Delta x) p_\Delta(\Delta x \mid x_n, \mu) d(\Delta x)}{\int_{\mathbb{R}^d} Q(z \mid \Delta x') p_\Delta(\Delta x' \mid x_n, \mu) d(\Delta x')}. \quad (\text{B.5})$$

This expression shows that the score is a ratio of weighted integrals over the displacement distribution.

This can be rewritten in a more interpretable form by defining the weight function:

$$w_\tau(z, \Delta x; x_n, \mu) := \frac{Q(z \mid \Delta x)}{\int_{\mathbb{R}^d} Q(z \mid \Delta x') p_\Delta(\Delta x' \mid x_n, \mu) d(\Delta x')}, \quad (\text{B.6})$$

which satisfies the normalization $\int w_\tau p_\Delta(\Delta x \mid x_n, \mu) d(\Delta x) = 1$.

With this notation, the score function becomes equation (14) in the main text. This representation reveals that the score function is a weighted average of “local scores” $-(z - \alpha_\tau \Delta x)/\beta_\tau^2$ over all possible displacement values, where the weights favor displacements that are more likely to have produced the current diffusion state z .